SUPPORTING INFORMATION

Why does Amazon precipitation decrease when tropical forests respond to increasing CO_2?

Submitted to Earth's Future

B. Langenbrunner[1], M. S. Pritchard[1], G. J. Kooperman[2], and J. T. Randerson[1]

[1]Department of Earth System Science, University of California, Irvine, Irvine, California, USA
[2]Department of Geography, University of Georgia, Athens, Georgia, USA

Contents

Table S1: Set of simulations for this study

Simulation	Resolution	Length of run	Ensemble size
WRF 50-km base set	50-km horizontal; 30 vertical levels	10 days	10
WRF 50-km sensitivity runs For schemes: YSU, MYJ, MYNN3, ACM2, UW, TEMF	50-km horizontal; 30 vertical levels	10 days	1 per scheme
WRF 50-10-2-km runs	Outer, intermediate, and small domains at 50-, 10-, and 2-km resolution with two-way nesting; 30 vertical levels	10 days	1
CESM short runs	2° finite volume	30 days	10
CESM long run	2° finite volume	10 years	1

WRF land surface model

An important requirement for these experiments is that the land model include vegetation physics in which stomata respond to CO2 concentrations. This study uses Noah-MP (**??**), which is an augmentation of the original Noah model (**??**) to more realistically represent certain biophysical and hydrologic processes. The important component is a Ball-Berry type stomatal conductance model (**????**), where conductance is inversely related to CO2 concentrations at the leaf surface. Note that Noah-MP also includes an option for a Jarvis-type parameterization scheme (**?**), though we have chosen to use the Ball-Berry option given its prominence in current land surface models. Early test simulations were performed with an alternative land model available in WRF, the Community Land Model version 4 (CLM4; **?**), and a similar response was observed in precipitation. In the main text, we present results for Noah-MP alone.

WRF boundary layer scheme

The YSU boundary layer scheme used here (**?**) plays a primary role in the land-atmosphere interactions that generate the physiological response. We introduce the main aspects below that are important in our results, though we refer the reader to the original publication for a full description.

This is a K-profile parameterization scheme (a nonlocal K approach) which evolved from **?** and accounts for nonlocal countergradient terms for vertical heat and momentum fluxes in large convective eddies in the boundary layer. This approach grew out of the need to include (nonlocal) deep convection in addition to the (local) unresolved turbulent activity to more accurately represent mixing processes through the full mixed layer (e.g., **?**). The K-profile strategy relies on specifying vertical profiles of diffusivity coefficients K (also referred to as eddy viscosities) that relate eddy covariances to resolved scale motions. The added value from the YSU parameterization is a more complex treatment of these entrainment processes at and above the boundary layer top.

The governing diffusion equation in YSU for , a prognostic variable, is given by

$$\frac{\partial c}{\partial t} = \frac{\partial}{\partial z}\left[K_c\left(\frac{\partial c}{\partial z} - \gamma_c\right) - \overline{(w'c')}_h\left(\frac{z}{h}\right)^3\right] \tag{1}$$

Here, c can represent winds u and v, potential temperature θ, or moisture q. The first term in brackets is the parameterized flux, where K_c is the eddy diffusivity coefficient acting on vertical gradients of c. γ_c is the nonlocal countergradient correction term that accounts for deep convective motions reaching the boundary layer top. The second term in brackets represents entrainment at the inversion layer and is a correction introduced by **?** to account for downward mixing above the boundary layer. $h$is the planetary boundary layer height, calculated using a bulk Richardson number threshold, and $\overline{(w'c')}_h$ is the flux of across the entrainment layer at this level, which is proportional to the change in c across the two model levels that surround h.

K_c takes on two values depending on which prognostic variable is being calculated: either K_t (t representing mass variables θ and q) or K_m (m representing momentum variables u and v). Given one, the other can be calculated using the Prandtl number Pr (the ratio of momentum to thermal diffusivity) as $K_t = K_m/\mathrm{Pr}$. To treat entrainment processes differently in the mixed layer, entrainment layer, and free troposphere, YSU first calculates K_m separately, and then derives K_t from the Prandtl number relationship.

In the mixed layer ($z < h$), this is done using the common formulation $K_m = kw_s z(1 - z/h)^p$. Here, k is the von Kármán constant ($= 0.4$), z is the height above ground level, h is the boundary layer height, and w_s is a velocity scale that depends on height and surface heat flux. This last term is what embeds nonlocal information about surface heat fluxes into the diffusivity coefficient.

When z falls within the entrainment layer, K_m and K_t depend on heat fluxes across it and follow calculations introduced by **?**. The width of this entrainment layer is on the order of tens of meters but can be influential in these fluxes. Above this layer ($z > h$), K_m is calculated as $K_m = l^2 f_m(\mathrm{Rig})|\partial U/\partial z|$, where l is a mixing length scale in the free atmosphere (**?**) and f_m is a function that depends on the gradient Richardson number Rig and is inversely related to its size.

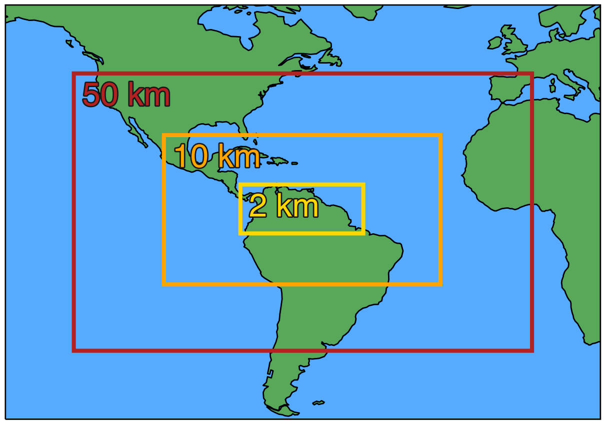

Figure S1: Nested domains for 50-10-2 km WRF simulations.

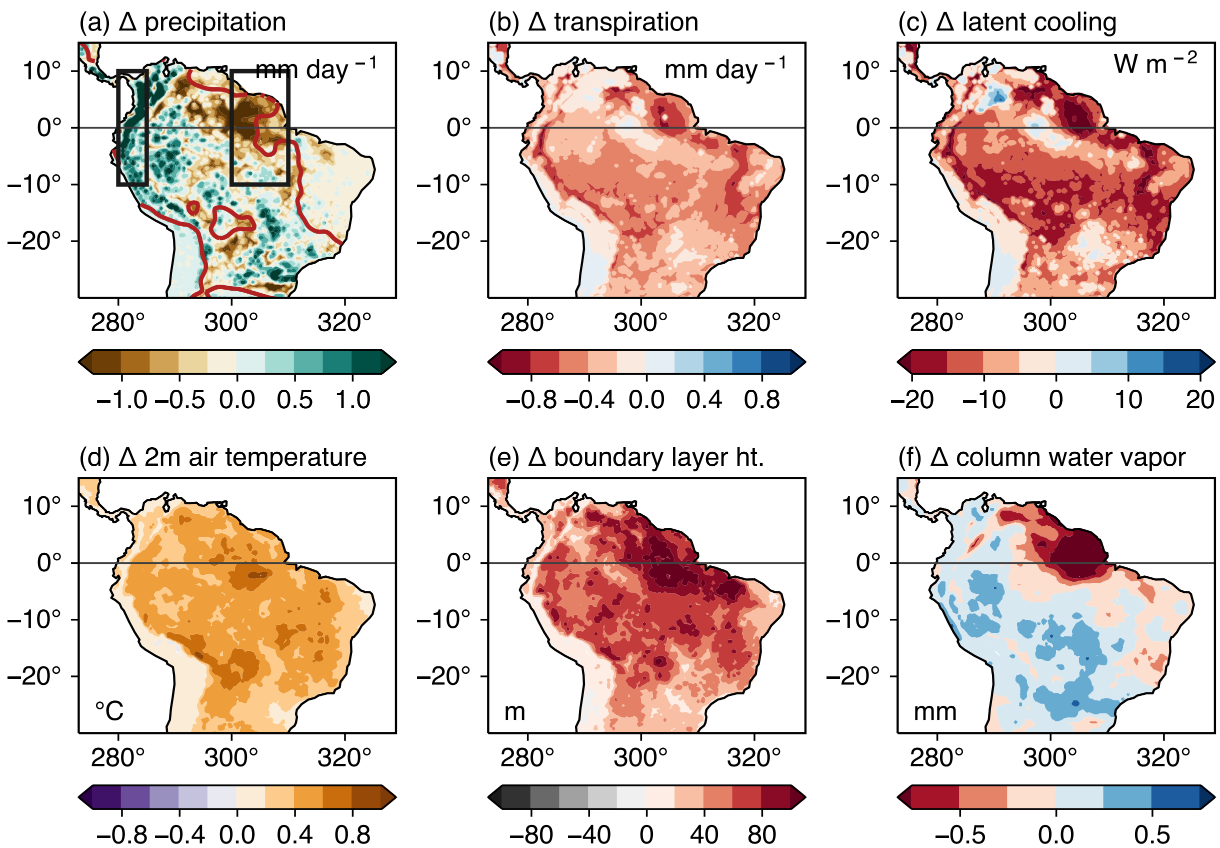

Figure S2: Ensemble mean change in absolute units ($CO_{2,phys}$–$CO_{2,cont}$) during days 2–10. Red lines in (a) show the 4 mm day^{-1} precipitation contours in $CO_{2,cont}$.

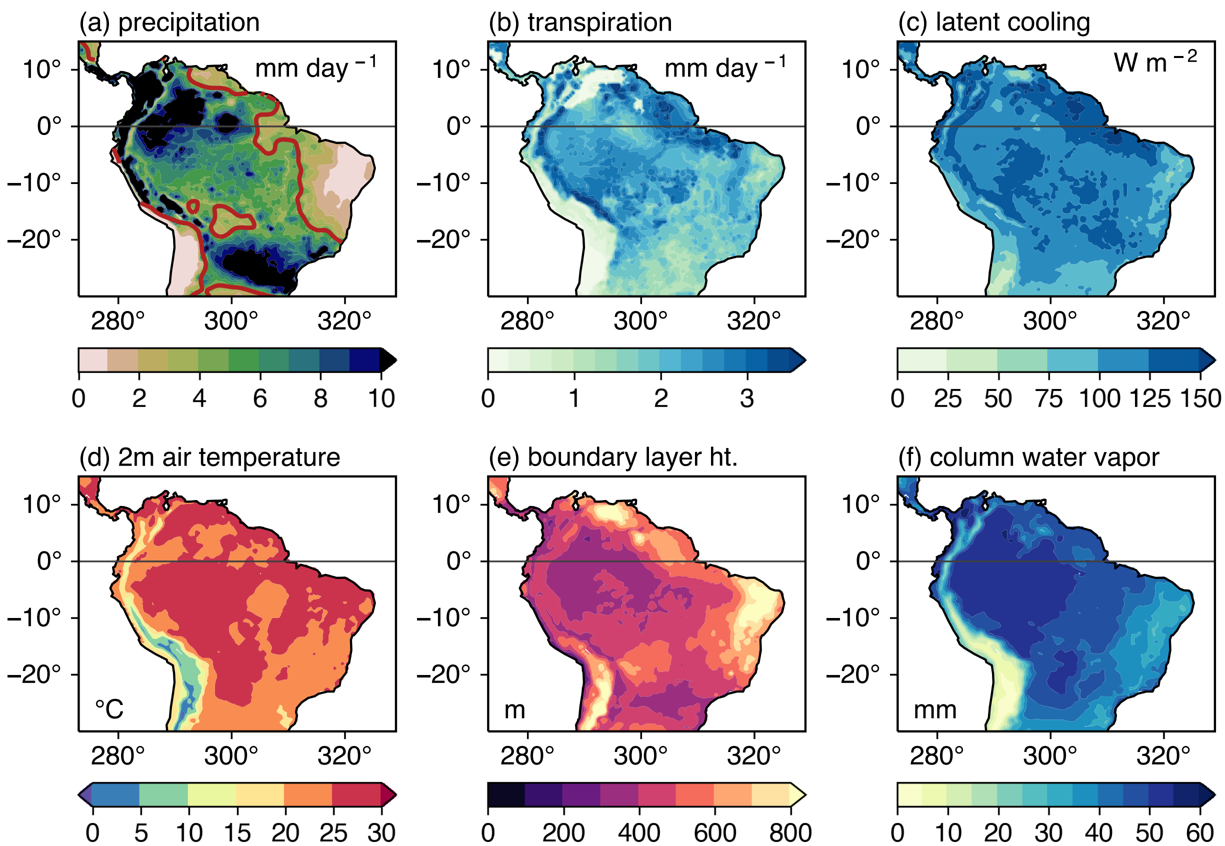

Figure S3: Ensemble mean for $CO_{2,cont}$ during days 2–10. Red lines in (a) show the 4 mm day^{-1} precipitation contours.

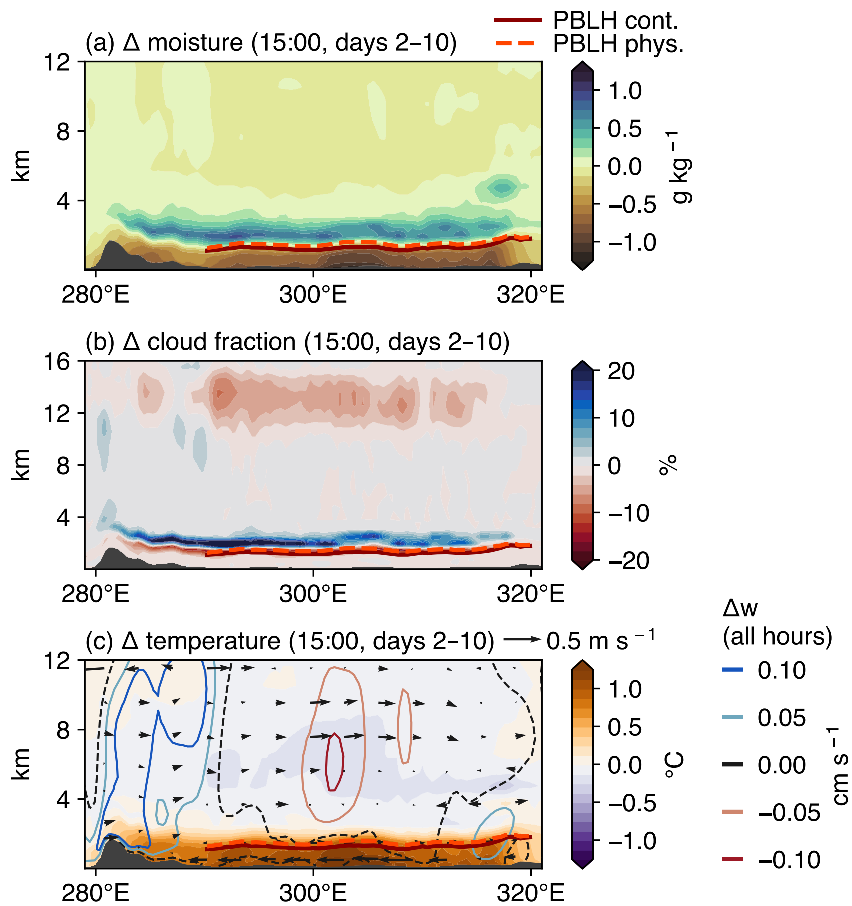

Figure S4: Ensemble mean WRF 50-km changes for $CO_{2,phys}$–$CO_{2,cont}$ at 15:00 for the full atmosphere during days 2–10. Contour lines in (c) show changes in vertical velocity averaged over the full diurnal cycle during days 2–10.

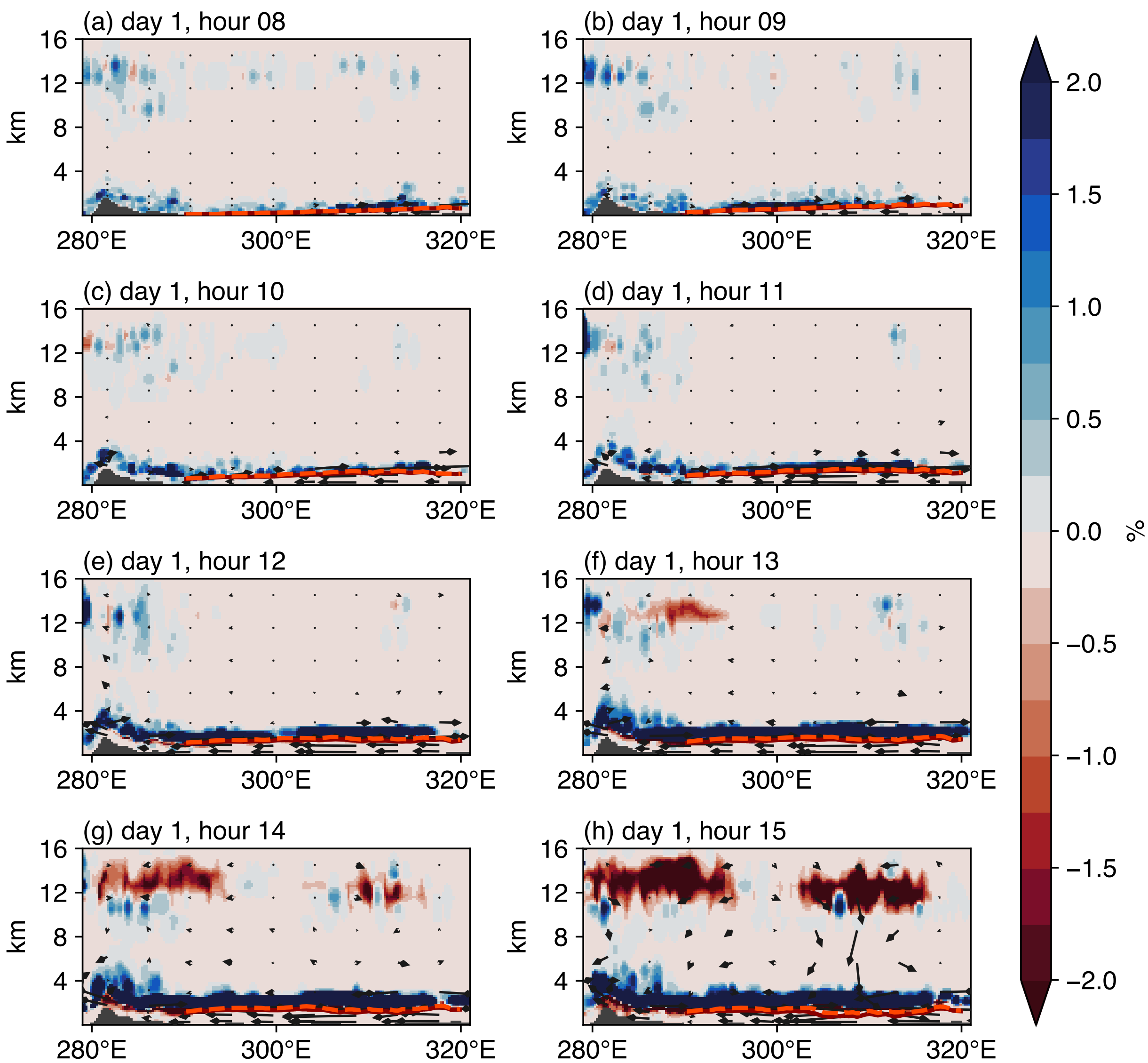

Figure S5: Ensemble mean change in cloud fraction for $CO_{2,phys}$–$CO_{2,cont}$ during 08:00–15:00 of day 1.

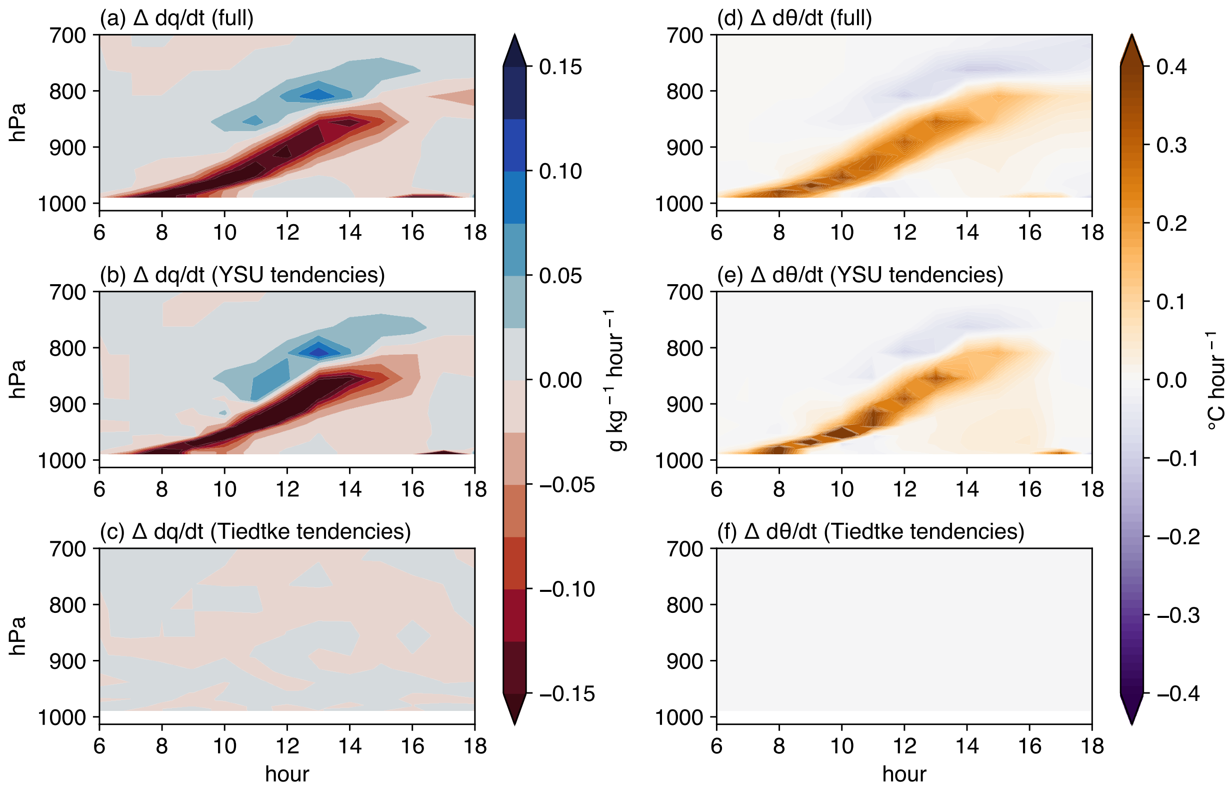

Figure S6: Changes ($CO_{2,phys}$–$CO_{2,cont}$) in moisture and potential temperature tendencies on day 1 of the 50-km YSU simulation. Plots here represent a single realization, not a forecast ensemble mean.

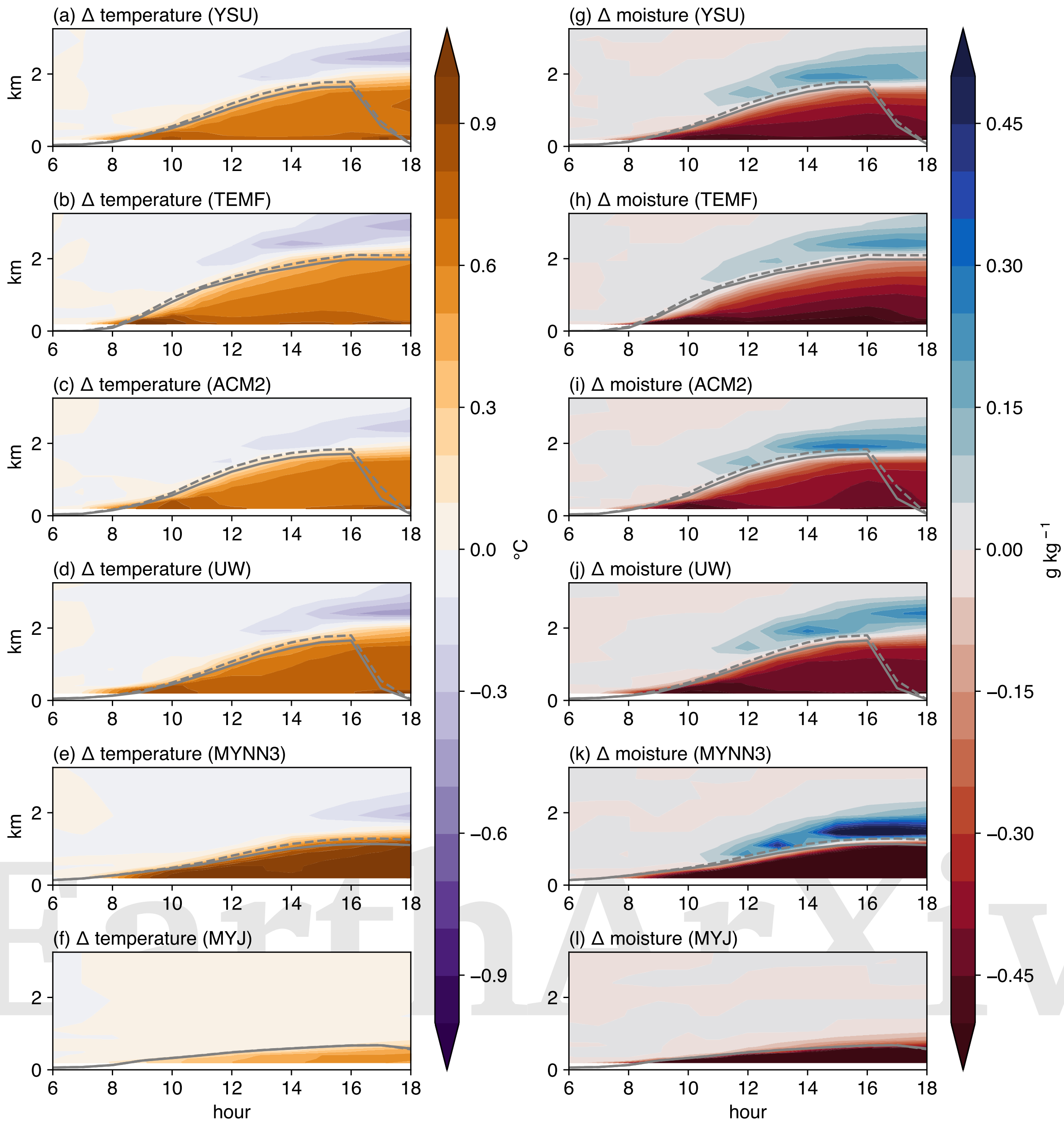

Figure S7: Sensitivity test of day 1 $CO_{2,phys}$–$CO_{2,cont}$ temperature and moisture anomalies over the Amazon region for the YSU boundary layer scheme as well as the TEMF, ACM2, UW, and MYNN3 schemes. Boundary layer heights as diagnosed by each scheme are shown for the control (solid) and physiological forcing (dashed) runs. Horizontal axis represents the local time on day 1. Each plot represents day 1 for a single realization, not a forecast ensemble.

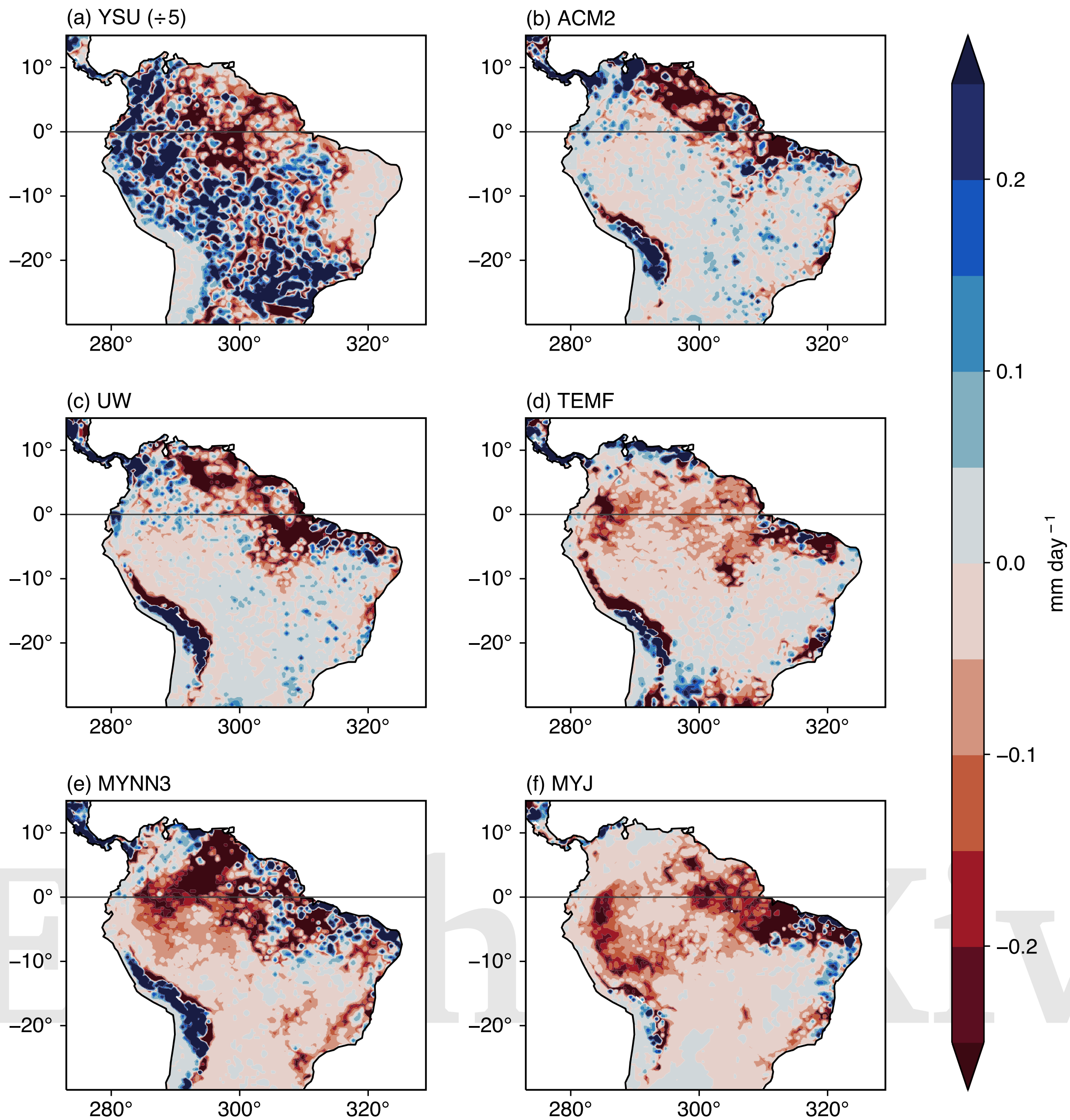

Figure S8: Mean $CO_{2,phys}$–$CO_{2,cont}$ precipitation change for each of six boundary layer schemes. Changes for YSU are larger than other simulations and have been divided by 5 for easier comparison. Each map represents days 2–10 for a single realization, not a forecast ensemble.

References